

Electronic Supplementary Information

Interfacial tension measurements using a new axisymmetric drop/bubble shape technique

M. A. Cabrerizo-Vilchez,[†] J. R. Fernández,[‡] M. A. Fernandez-Rodriguez,[¶] L. García-Río,^{*,§} M. Carmen Muñiz,^{*,||} and Cristina Núñez[⊥]

[†]*Biocolloid and Fluid Physics Group, Applied Physics Department, Faculty of Sciences, University of Granada, Avda. de la Fuente Nueva s/n, E-18071 Granada, Spain.*

[‡]*Department of Applied Mathematics, University of Vigo, Campus Universitario As Lagoas Marcosende s/n, E-36310 Vigo, Spain.*

[¶]*Laboratory for Interfaces, Soft Matter and Assembly, Department of Materials, ETH Zurich - Vladimir-Plelog-Weg 5 E-8093 Zurich, Switzerland.*

^{*}*Centro de Investigación en Química Biolóxica e Materiais Moleculares, Departamento de Química Física, Universidade de Santiago de Compostela, Campus Vida s/n, E-15782 Santiago de Compostela, Spain.*

^{||}*Departamento de Matemática Aplicada, Universidade de Santiago de Compostela, Campus Vida s/n, E-15782 Santiago de Compostela, Spain.*

[⊥]*Departamento de Didácticas Aplicadas, Área de Didáctica de la Matemática, Universidade de Santiago de Compostela, Campus Norte s/n, E-15782 Santiago de Compostela, Spain.*

E-mail: luis.garcia@usc.es; mcarmen.muniz@usc.es

Contents

1. Scheme of pendant bubble device	3
2. Parametrization of the surface of revolution and its mean curvature	4
3. Discretization of the Young-Laplace equation	6
4. Sessile drops	10
5. Air bubbles as function of time	12
6. Radius and surface tension of an air bubble in a water solution calculated with ADSA and PRO2TEN as a function of time	13
7. Radius and surface tension of air bubbles in a decanol solution with dif- ferent concentrations calculated with ADSA and PRO2TEN as a function of time	14

1. Scheme of pendant bubble device

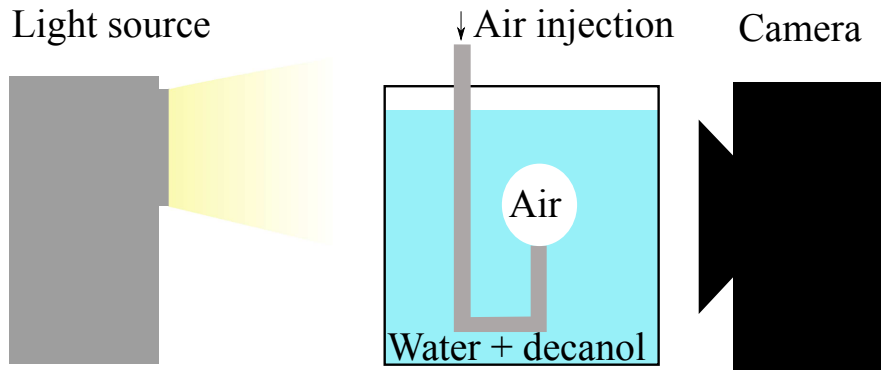


Figure S1: Scheme of the pendant bubble device.

New numerical method for surface tension determination.

2. Parametrization of the surface of revolution and its mean curvature

We assume that the interface, denoted by S , is a surface of revolution by applying a rotation about the z -axis, see Figure 1 (b) in the paper, which is parametrized by the following map

$$\begin{aligned} \mathbf{X} : [\theta_a, \theta_c] \times [0, 2\pi] &\longrightarrow S \\ (\theta, \varphi) &\longrightarrow \mathbf{X}(\theta, \varphi) = (y(\theta) \cos \varphi, y(\theta) \sin \varphi, z(\theta)) \end{aligned}$$

where $y(\theta) = r(\theta) \sin \theta$ and $z(\theta) = r(\theta) \cos \theta$ and $0 < \theta_a < \theta_c < \pi$.

From the surface parametrization \mathbf{X} , we obtain the first derivatives

$$\begin{aligned} \mathbf{X}_\theta &= (y'(\theta) \cos \varphi, y'(\theta) \sin \varphi, z'(\theta)), \\ \mathbf{X}_\varphi &= (-y(\theta) \sin \varphi, y(\theta) \cos \varphi, 0), \end{aligned}$$

and we calculate its cross product

$$\mathbf{X}_\theta \times \mathbf{X}_\varphi = (-y(\theta) z'(\theta) \cos \varphi, -y(\theta) z'(\theta) \sin \varphi, y(\theta) y'(\theta)).$$

The coefficients of the first fundamental forms are straightforwardly determined by

$$\begin{aligned} E &= \mathbf{X}_\theta \cdot \mathbf{X}_\theta = y'(\theta)^2 + z'(\theta)^2, \\ F &= \mathbf{X}_\theta \cdot \mathbf{X}_\varphi = 0, \\ G &= \mathbf{X}_\varphi \cdot \mathbf{X}_\varphi = y(\theta)^2. \end{aligned}$$

Using the cross product of the first derivatives, we find that the inner unit normal vector to

the surface is

$$\mathbf{n} = \left(\frac{z'(\theta) \cos \varphi}{\sqrt{z'(\theta)^2 + y'(\theta)^2}}, \frac{z'(\theta) \sin \varphi}{\sqrt{z'(\theta)^2 + y'(\theta)^2}}, -\frac{y'(\theta)}{\sqrt{z'(\theta)^2 + y'(\theta)^2}} \right),$$

and, using this vector, we obtain the coefficients of the second fundamental form

$$\begin{aligned} L &= \mathbf{X}_{\theta\theta} \cdot \mathbf{n} = \frac{y''(\theta) z'(\theta)}{\sqrt{z'(\theta)^2 + y'(\theta)^2}} - \frac{y'(\theta) z''(\theta)}{\sqrt{z'(\theta)^2 + y'(\theta)^2}}, \\ M &= \mathbf{X}_{\theta\varphi} \cdot \mathbf{n} = 0, \\ N &= \mathbf{X}_{\varphi\varphi} \cdot \mathbf{n} = -\frac{y(\theta) z'(\theta)}{\sqrt{z'(\theta)^2 + y'(\theta)^2}}. \end{aligned}$$

Now, taking into account that the mean curvature of X , H , is given by the expression

(see¹)

$$H = \frac{1}{2} \frac{LG - 2MF + NE}{EG - F^2},$$

we have

$$H = \frac{1}{2} \frac{y(\theta) (y''(\theta) z'(\theta) - y'(\theta) z''(\theta)) - z'(\theta) (y'(\theta)^2 + z'(\theta)^2)}{y(\theta) (y'(\theta)^2 + z'(\theta)^2)^{3/2}}.$$

3. Discretization of the Young-Laplace equation

Both the function $r(\cdot)$ and the constant C in equation (8) in the paper are the unknowns of our problem. Assuming the radial section of the interface to be polygonal, we consider a uniform partition of the interval $[\theta_a, \theta_c]$, denoted by $\theta_a = \theta_1 < \theta_2 < \dots < \theta_{N+1} = \theta_c$. Then, we have a partition with step size $h = (\theta_c - \theta_a)/N$ and $N + 1$ nodes given by

$\theta_n = \theta_1 + (n - 1)h$, for $n = 1, \dots, N + 1$, and we look for the constant C and the set of

radii $\{r_n\}_{n=1}^N$ such that

$$r_n = r(\theta_n), \quad n = 1, \dots, N. \quad (1)$$

Notice that the value of $r_{N+1} = r(\theta_{N+1})$ is not an unknown since it is given by the boundary condition (10) written in the paper, that is to say, $r_{N+1} = r_c$.

Now, we define the following mapping $G : \mathbb{R}^{N+1} \rightarrow \mathbb{R}^{N+1}$ by

$$G(\bar{r}) = (G_1(\bar{r}), \dots, G_{N+1}(\bar{r})),$$

where

$$\bar{r} = (r_1, \dots, r_N, C),$$

and

$$G_i(\bar{r}) = 2(H_d(\bar{r}))_i - \frac{\rho g}{\gamma} r_i \cos \theta_i - C, \quad i = 1, \dots, N, \quad (2)$$

$$G_{N+1}(\bar{r}) = \frac{2\pi h}{9} \left(r_1^3 \sin \theta_1 + 4 \sum_{i=1}^{N/2} r_{2i}^3 \sin \theta_{2i} + 2 \sum_{i=2}^{N/2} r_{2i-1}^3 \sin \theta_{2i-1} + r_c^3 \sin \theta_{N+1} \right) - V. \quad (3)$$

H_d denotes in (2) the discrete approximation of the mean curvature given by

$$(H_d(\bar{r}))_i = \frac{1}{2} \frac{y(\theta_i)(z_1(\bar{r})_i y_2(\bar{r})_i - z_2(\bar{r})_i y_1(\bar{r})_i) - z_1(\bar{r})_i(y_1(\bar{r})_i^2 + z_1(\bar{r})_i^2)}{y(\theta_i)(y_1(\bar{r})_i^2 + z_1(\bar{r})_i^2)^{3/2}},$$

where $y(\theta_i) = r_i \sin \theta_i$, $y_1(\bar{r})_i$ and $y_2(\bar{r})_i$ being the following approximation of the first and second derivatives of y at θ_i , respectively,

$$\begin{aligned} y_1(\bar{r})_i &= \frac{y(\theta_{i+1}) - y(\theta_{i-1})}{2h}, \\ y_2(\bar{r})_i &= \frac{y(\theta_{i+1}) - 2y(\theta_i) + y(\theta_{i-1})}{h^2}. \end{aligned}$$

Analogously, $z(\theta_i) = r_i \cos \theta_i$, $z_1(\bar{r})_i$ and $z_2(\bar{r})_i$ are the approximations of the first and second derivatives of z at θ_i , respectively. Therefore

$$\begin{aligned} z_1(\bar{r})_i &= \frac{z(\theta_{i+1}) - z(\theta_{i-1})}{2h}, \\ z_2(\bar{r})_i &= \frac{z(\theta_{i+1}) - 2z(\theta_i) + z(\theta_{i-1})}{h^2}. \end{aligned}$$

Taking into account the boundary conditions (9) and (10) given in the paper, we take $r_{-1} = r_1$ and $r_{N+1} = r_c$, respectively. Finally, equation (3) stands for the composite Simpson's rule to compute the volume.

Notice that (2) is the discrete version of the equilibrium equation (8) (given in the paper) at every node of the partition. The interface profile is achieved for a $\bar{r} \in \mathbb{R}^{N+1}$ such that $G(\bar{r}) = \mathbf{0}$. In order to do that, we use the Newton method, so we have the following expression

$$\bar{r}^{m+1} = \bar{r}^m - D G(\bar{r}^m)^{-1} G(\bar{r}^m), \quad (4)$$

DG being the Jacobian matrix. For obtaining the solution to (4), we proceed as follows

$$\bar{r}^{m+1} = \bar{r}^m + \delta,$$

δ being the solution of the linear system

$$DG(\bar{r}^m) \delta = -G(\bar{r}^m). \quad (5)$$

We notice that DG is a $(N+1) \times (N+1)$ -matrix which can be written in terms of blocks as follows

$$DG = \left(\begin{array}{c|c} T & A \\ \hline B & 0 \end{array} \right),$$

T being a tridiagonal $N \times N$ -matrix such that $T_{ij} = \frac{\partial G_i}{\partial r_j}(\bar{r})$, for $i, j = 1, \dots, N$, A is a $N \times 1$ -matrix of ones and B is a $1 \times N$ -matrix.

Then, linear system (5) reads

$$\left(\begin{array}{c|c} T & A \\ \hline B & 0 \end{array} \right) \left(\begin{array}{c} \alpha \\ \hline \delta_{N+1} \end{array} \right) = \left(\begin{array}{c} \beta \\ \hline -G_{N+1}(\bar{r}^m) \end{array} \right),$$

where $\alpha = (\delta_1, \dots, \delta_N)^t$ and $\beta = (-G_1(\bar{r}^m), \dots, -G_N(\bar{r}^m))^t$. Therefore, from the previous system, we have

$$T\alpha + A\delta_{N+1} = \beta,$$

$$B\alpha = -G_{N+1}(\bar{r}^m),$$

which is solved using the following algorithm:

- Compute p_1 the solution of the linear system $T p_1 = \beta$.

- Compute p_2 the solution of the linear system $T p_2 = A$.
- $\delta_{N+1} = (-G_{N+1}(\bar{r}^m) - B p_1)/(-B p_2)$.
- $\alpha = p_1 - p_2 \delta_{N+1}$.

4. Sessile drops

Using the data $\gamma = 0.01809 \text{ N/m}$ and $R_a = 0.002 \text{ m}$, a theoretical drop of $6 \mu\text{l}$ is obtained. Its volume, the coordinates of the contact point, ρ , g and γ are the input parameters of the numerical code TEN2PRO its output parameters being the profile of the drop and the curvature at the apex. Both the theoretical and numerical profiles are shown in Figure S2. Analogously, theoretical drops of $10 \mu\text{l}$ and $20 \mu\text{l}$ are obtained for the data $\gamma = 0.039 \text{ N/m}$ and $\gamma = 0.09 \text{ N/m}$, respectively. Their respective volumes, coordinates of the contact point and tension are the input parameters of the numerical code TEN2PRO A section of a sphere is the initial profile in the Newton algorithm.

The profile of the numerical drop are also shown in Figure S2. In Table S1 the relative error between numerical and theoretical sessile drops —denoted by num and th superscripts, respectively—is presented in terms of the size of the partition N :

$$E_r^2 = \sum_{i=1}^N \left(\frac{r_i^{th} - r_i^{num}}{r_i^{th}} \right)^2. \quad (6)$$

Table S1: Relative error for sessile drops

N	$E_r (V = 6 \mu\text{l})$	$E_r (V = 10 \mu\text{l})$	$E_r (V = 20 \mu\text{l})$
60	1.88×10^{-3}	1.49×10^{-3}	1.25×10^{-3}
120	6.04×10^{-4}	4.90×10^{-4}	4.26×10^{-4}
240	1.47×10^{-4}	1.04×10^{-4}	1.20×10^{-4}

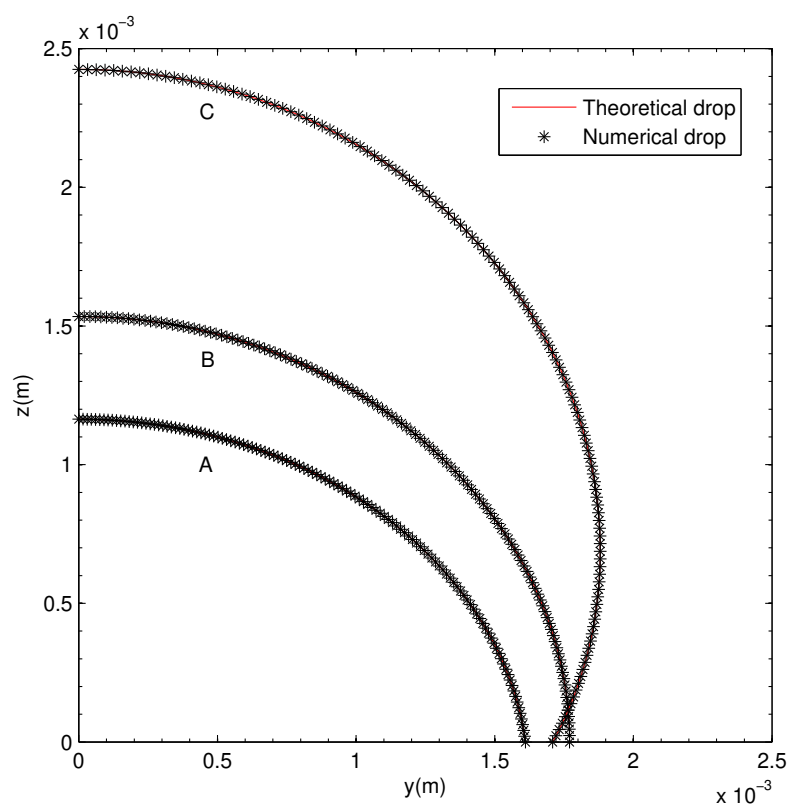


Figure S2: Sessile drop profiles of theoretical and numerical drops. A: $V = 6 \mu\text{l}$, B: $V = 10 \mu\text{l}$, C: $V = 20 \mu\text{l}$.

5. Air bubbles as function of time



Figure S3: Three air bubbles of $35 \mu\text{l}$ into $8.3 \times 10^{-8}\text{mol}/\text{cm}^3$ decanol solution at $t=10 \text{ s}$, 100 s and 1000 s .

6. Radius and surface tension of an air bubble in a water solution calculated with ADSA and PRO2TEN as a function of time

Table S2: Air bubble into water.

Time (s)	R_a (m) ADSA	γ (N/m) ADSA	R_a (m) PRO2TEN	γ (N/m) PRO2TEN
1.12	0.001780	0.07266	0.001784	0.07272
5.19	0.001780	0.07203	0.001781	0.07204
90	0.001780	0.07207	0.001781	0.07211
100	0.001780	0.07210	0.001781	0.07207
500	0.001780	0.07198	0.001780	0.07181
800	0.001780	0.07202	0.001780	0.07182
901	0.001781	0.07215	0.001781	0.07198
1000	0.001780	0.07213	0.001780	0.07200
1101	0.001780	0.07207	0.001781	0.07197
1200	0.001780	0.07203	0.001780	0.07195

7. Radius and surface tension of air bubbles in a decanol solution with different concentrations calculated with ADSA and PRO2TEN as a function of time

Table S3: Decanol aqueous solutions, 1.6×10^{-7} mol/cm³.

Time (s)	R_a (m) ADSA	γ (N/m) ADSA	R_a (m) PRO2TEN	γ (N/m) PRO2TEN
5	0.001478	0.04502	0.001487	0.04642
10	0.001456	0.04194	0.001464	0.04272
21	0.001438	0.03985	0.001441	0.03957
41	0.001424	0.03823	0.001427	0.03806
80	0.001407	0.03669	0.001400	0.03531
100	0.001402	0.03622	0.001400	0.03518
201	0.001394	0.03561	0.001396	0.03501
300	0.001396	0.03675	0.001410	0.03863
400	0.001396	0.03669	0.001406	0.03824
600	0.001394	0.03655	0.001410	0.03845
801	0.001395	0.03687	0.001409	0.03890
1002	0.001396	0.03690	0.001410	0.03902
1200	0.001398	0.03716	0.001415	0.03952

Table S4: Decanol aqueous solutions, 1.2×10^{-7} mol/cm³.

Time (s)	R_a (m) ADSA	γ (N/m) ADSA	R_a (m) PRO2TEN	γ (N/m) PRO2TEN
5	0.001514	0.05109	0.001522	0.05230
10	0.001497	0.04806	0.001507	0.04942
20	0.001482	0.04558	0.001489	0.04642
40	0.001471	0.04405	0.001478	0.04439
80	0.001461	0.04265	0.001462	0.04215
100	0.001458	0.04220	0.001462	0.04191
200	0.001451	0.04146	0.001453	0.04061
300	0.001449	0.04117	0.001450	0.04023
400	0.001447	0.04098	0.001442	0.03936
600	0.001448	0.04109	0.001453	0.04076
800	0.001447	0.04099	0.001449	0.04032
1000	0.001447	0.04098	0.001449	0.04034
1200	0.001447	0.04094	0.001449	0.04028

Table S5: Decanol aqueous solutions, 8.3×10^{-8} mol/cm³.

Time (s)	R_a (m) ADSA	γ (N/m) ADSA	R_a (m) PRO2TEN	γ (N/m) PRO2TEN
5	0.001724	0.06814	0.001733	0.07037
10	0.001704	0.06460	0.001714	0.06683
20	0.001671	0.05962	0.001676	0.06035
40	0.001638	0.05551	0.001641	0.05586
80	0.001613	0.05299	0.001610	0.05239
100	0.001606	0.05226	0.001603	0.05159
200	0.001588	0.05078	0.001580	0.04953
300	0.001579	0.05011	0.001569	0.04881
401	0.001574	0.04979	0.001569	0.04872
600	0.001570	0.04954	0.001561	0.04816
800	0.001568	0.04941	0.001561	0.04809
1000	0.001568	0.04940	0.001560	0.04801
1200	0.001568	0.04940	0.001561	0.04808

 Table S6: Decanol aqueous solutions, 4.7×10^{-8} mol/cm³.

Time (s)	R_a (m) ADSA	γ (N/m) ADSA	R_a (m) PRO2TEN	γ (N/m) PRO2TEN
5	0.001773	0.07122	0.001779	0.07242
10	0.001772	0.07100	0.001777	0.07212
20	0.001767	0.07012	0.001776	0.07174
40	0.001751	0.06770	0.001776	0.06920
90	0.001696	0.06063	0.001691	0.05989
100	0.001695	0.06044	0.001691	0.05985
200	0.001672	0.05827	0.001666	0.05738
300	0.001661	0.05737	0.001656	0.05631
400	0.001657	0.05706	0.001648	0.05563
600	0.001655	0.05686	0.001644	0.05537
800	0.001653	0.05671	0.001645	0.05530
1000	0.001652	0.05673	0.001644	0.05522
1210	0.001652	0.05673	0.001644	0.05526

References

- (1) A. Pressley, *Elementary Differential Geometry*, Springer – Verlag, London, 2001.